

CYCLOTRON HARMONICS IN ACCRETING PULSARS AND GAMMA-RAY BURSTERS:  
EFFECT OF TWO-PHOTON PROCESSES

S. G. ALEXANDER AND P. MÉSZÁROS

Department of Astronomy and Astrophysics, 525 Davey Laboratory, Pennsylvania State University, University Park, PA 16802

Received 1990 May 9; accepted 1990 August 24

## ABSTRACT

We discuss the radiative transfer at the cyclotron first, second, and third harmonics for simplified accreting pulsar and gamma-ray burster emission regions. We include two-photon scattering as well as two-photon emission, which play a major role in determining the line-strength ratio. Stimulated effects are also important for accurately modeling the optically thick line and continuum regions. These calculations are compared with recent observations of accreting pulsars and gamma-ray burst sources, showing a qualitative agreement. We find that the cyclotron harmonic lines should be strongly polarized.

*Subject headings:* gamma rays: bursts — line formation — pulsars — radiation mechanisms — radiative transfer — stars: accretion — stars: magnetic — X-rays: binaries — X-rays: spectra

## 1. INTRODUCTION

The recent observation of cyclotron lines in several accreting X-ray pulsars with the *Ginga* spacecraft large-area proportional counters (4U 1538–52: Clark et al. 1990; Her X-1: Mihara et al. 1990; NGC 6712: Roussel-Dupré et al. 1990; X0331+63: Makishima et al. 1991; 4U 0115+63: Nagase et al. 1991) confirms and expands the previous similar observations with other instruments (Her X-1: Trümper et al. 1978; 4U 0115+63: Wheaton et al. 1979, White, Swank, & Holt 1983). A different set of instruments on board *Ginga*, the gamma burst detector (GBD), have also found strong evidence for cyclotron lines in several gamma-ray bursters, GB 880205 and GB 870303 (Murakami et al. 1988; Fenimore et al. 1988), and GB 890929 (Yoshida et al. 1990). These strengthen the earlier reports of cyclotron lines in gamma-ray bursters obtained with the KONUS detector on the *Venera 11* and *Venera 12* spacecraft (Mazets et al. 1982 and references therein). These observations have provided a great impetus for attempts at modeling the emission region of these objects, and in particular at understanding the physical properties of the cyclotron line-emitting plasma. Such models are necessary for obtaining information about the field strength, the plasma optical depth, and the temperature, which can then be used for setting limits on the luminosity and distance of the source, as well as the accretion rate.

While a complete model of the dynamics and energy deposition mechanism is still lacking, simple static models of accreting X-ray pulsars (AXPs) have been developed to model the continuum, line emission, and pulse shapes (e.g., Mészáros & Nagel 1985a, b), using the magnetic single-photon scattering in the nonrelativistic approximation and neglecting stimulated effects, with a discrete ordinate Feautrier polarized transfer code. This incorporates Comptonization effects in an angle-dependent manner, and is suited for investigating polarized angle-dependent line and continuum spectra and pulse shapes. Monte Carlo studies of the Comptonization effects in the line were performed by Wang, Wasserman, & Salpeter (1988, 1989a), using nonrelativistic cross sections with relativistic kinematics included. Higher cyclotron harmonics and two-photon effects were not included in these earlier AXP atmosphere calculations. The effects of the relativistic magnetic single-photon scattering and of stimulated effects was discussed in Alexander, Mészáros, & Bussard (1989), where an extension of the Feautrier method is discussed for dealing with the nonlinearities associated with stimulated scattering. This used the relativistic cross sections calculated in Bussard, Alexander, & Mészáros (1986), which, similar to the work of Daugherty & Harding (1986), investigated both the single-photon and the two-photon scattering involving an excited final electron state. Two-photon scattering was investigated in the framework of gamma-ray bursters (GRBs) by Harding & Preece (1989), Wang et al. (1989b), and Alexander & Mészáros (1989), using a phenomenological model of a cold gas sheet illuminated by a power law gamma-ray spectrum. In these papers it was found that the two-photon scattering has a major effect in controlling the depth of the first harmonic relative to the second and higher harmonics. There is in addition another effect which is of the same order as the single-photon and two-photon scattering, which has thus far been neglected in QED calculations. This is the magnetic two-photon emission process (Alexander & Mészáros 1990a, b), which should be included with the other two processes in a consistent radiative transfer calculation.

In this paper we investigate the magnetic radiative transfer problem using a Feautrier transfer code that incorporates the relativistic one- and two-photon scattering, two-photon emission, and stimulated scattering effects. The polarization of the plasma as well as that of the vacuum is included, and we consider harmonics up to and including the third, for plasma parameters similar to those found in accreting X-ray pulsars and in the sheet model of gamma-ray bursters. Since the two-photon effects introduce a nonlinearity in the transfer equations, as do the stimulated scattering effects, we use the linearization method of the Feautrier equations described in Alexander et al. (1989), and solve the system of matrix equations by iterations. The inclusion of these new physical effects in the relativistic form requires a rather large computational setup. Because we are here interested in understanding the physics of the cyclotron line-forming region, and exploring the relative importance of the various effects, for computational convenience we use one typical angle of scattering, as in the two-stream approximation (Chandrasekhar 1960). This gives results which are close to those of an angle-averaged or diffusion approximation. In § 2 we describe the discretized form of the one-photon and two-photon scattering and two-photon emission redistribution functions introduced in Alexander & Mészáros (1990b, here-

after Paper I), as well as the corresponding photon source terms. In § 3 we describe the numerical computations on a model atmosphere of parameters similar to those expected in the AXP Hercules X-1, and look at the effect of consecutively switching on the various physical processes mentioned above. In § 5 we discuss the implications for future model calculations of AXP and GRB emission regions, and the implications for observed sources.

## 2. METHOD OF CALCULATION

In Paper I the cross sections for the processes of two-photon scattering and emission were calculated and were shown to be nonlinear in photon occupation number even if stimulated factors are neglected. This presents a serious complication if one wants to include these processes in a solution of the radiative transport equation. A numerical method has been developed (see Alexander et al. 1989) that is an extension of the well-known Feautrier technique that includes nonlinear terms and solves the differential equation of radiative transport by iteration. We will employ this method here to calculate flux spectra that include the higher cyclotron harmonics for slab models of accreting X-ray pulsars.

Before any solutions of the nonlinear radiative transport equation are attempted, the scattering opacities and sources from Paper I must be linearized according to the prescription in Alexander et al. (1989). That is, for each scattering process, the substitution is made for the photon occupation number  $N_\alpha = N_\alpha^0 + \delta N_\alpha$ , where  $N_\alpha^0$  is a known photon distribution and  $\delta N_\alpha$  is a small perturbation. Then  $\kappa_\alpha^0$  and  $Q_\alpha^0$  are those parts of the opacities and sources that are independent of  $\delta N_\alpha$ , while the perturbations can be respectively written as

$$\delta\kappa_\alpha = \sum_{\alpha'} E_{\alpha\alpha'} \delta N_{\alpha'}, \quad (1)$$

$$\delta Q_\alpha = \sum_{\alpha'} F_{\alpha\alpha'} \delta N_{\alpha'}, \quad (2)$$

where  $\alpha$  stands for the set of photon parameters, frequency, direction, and polarization. Here, in contrast to the notation of Paper I, a discrete ordinate basis is used so that the redistribution functions become matrices, and the integration over photon states  $\alpha$  becomes a quadrature sum over frequencies, angles, and polarizations.

The expressions for the scattering opacities and sources are derived in Paper I. For one-photon Compton scattering, the linearization procedure gives

$$Q_{C,\alpha}^0 = \sum_{\alpha'} N_\alpha^0 e^{(\omega' - \omega)/T} \mathcal{R}_{\alpha\alpha'}, \quad (3)$$

$$\kappa_{C,\alpha}^0 = \sum_{\alpha'} (1 + k_{\text{st}} N_\alpha^0) \mathcal{R}_{\alpha\alpha'} - k_{\text{st}} Q_{C,\alpha}^0, \quad (4)$$

$$F_{C,\alpha\alpha'} = e^{(\omega' - \omega)/T} \mathcal{R}_{\alpha\alpha'}, \quad (5)$$

$$E_{C,\alpha\alpha'} = k_{\text{st}} (\mathcal{R}_{\alpha\alpha'} - F_{C,\alpha\alpha'}), \quad (6)$$

where  $k_{\text{st}}$  is a numerical switch that equals 1 (0) to include (not include) stimulated effects. Linearization of the two-photon scattering direct process terms yields, for the terms labeled as 1x,

$$Q_{1x,\alpha}^0 = \sum_{\alpha'} N_\alpha^0 \sum_{\alpha''} N_{\alpha''}^0 e^{(\omega' + \omega'' - \omega)/T} \mathcal{X}_{\alpha\alpha'\alpha''}, \quad (7)$$

$$\kappa_{1x,\alpha}^0 = \sum_{\alpha'} (1 + k_{\text{st}} N_\alpha^0) \sum_{\alpha''} (1 + k_{\text{st}} N_{\alpha''}^0) \mathcal{X}_{\alpha\alpha'\alpha''} - k_{\text{st}} Q_{1x,\alpha}^0, \quad (8)$$

$$F_{1x,\alpha\alpha'} = \sum_{\alpha''} N_{\alpha''}^0 e^{(\omega' + \omega'' - \omega)/T} (\mathcal{X}_{\alpha\alpha'\alpha''} + \mathcal{X}_{\alpha\alpha''\alpha'}), \quad (9)$$

$$E_{1x,\alpha\alpha'} = k_{\text{st}} \sum_{\alpha''} (1 + N_{\alpha''}^0) (\mathcal{X}_{\alpha\alpha'\alpha''} + \mathcal{X}_{\alpha\alpha''\alpha'}) - k_{\text{st}} F_{1x,\alpha\alpha'}; \quad (10)$$

for the inverse 2x terms,

$$Q_{2x,\alpha}^0 = \sum_{\alpha'} N_\alpha^0 \sum_{\alpha''} (1 + k_{\text{st}} N_{\alpha''}^0) \mathcal{X}'_{\alpha'\alpha''\alpha}, \quad (11)$$

$$\kappa_{2x,\alpha}^0 = \sum_{\alpha'} N_\alpha^0 \sum_{\alpha''} (1 + k_{\text{st}} N_{\alpha''}^0) e^{(\omega + \omega' - \omega'')/T} \mathcal{X}'_{\alpha'\alpha''\alpha} - k_{\text{st}} Q_{2x,\alpha}^0, \quad (12)$$

$$F_{2x,\alpha\alpha'} = \sum_{\alpha''} [(1 + k_{\text{st}} N_{\alpha''}^0) \mathcal{X}'_{\alpha'\alpha''\alpha} + k_{\text{st}} N_{\alpha''}^0 \mathcal{X}'_{\alpha''\alpha'\alpha}], \quad (13)$$

$$E_{2x,\alpha\alpha'} = \sum_{\alpha''} [(1 + k_{\text{st}} N_{\alpha''}^0) e^{(\omega + \omega' - \omega'')/T} \mathcal{X}'_{\alpha'\alpha''\alpha} + k_{\text{st}} N_{\alpha''}^0 e^{(\omega + \omega' - \omega'')/T} \mathcal{X}'_{\alpha''\alpha'\alpha}] - k_{\text{st}} F_{2x,\alpha\alpha'}; \quad (14)$$

and those terms labeled 3x (i.e., photon exchange of the inverse),

$$Q_{3x,\alpha}^0 = \sum_{\alpha'} N_\alpha^0 \sum_{\alpha''} (1 + k_{\text{st}} N_{\alpha''}^0) \mathcal{X}'_{\alpha'\alpha\alpha''}, \quad (15)$$

$$\kappa_{3x,\alpha}^0 = \sum_{\alpha'} N_\alpha^0 \sum_{\alpha''} (1 + k_{\text{st}} N_{\alpha''}^0) e^{(\omega' + \omega - \omega'')/T} \mathcal{X}'_{\alpha'\alpha\alpha''} - k_{\text{st}} Q_{3x,\alpha}^0, \quad (16)$$

$$F_{3x,\alpha\alpha'} = \sum_{\alpha''} [(1 + k_{\text{st}} N_{\alpha''}^0) \mathcal{X}'_{\alpha'\alpha\alpha''} + k_{\text{st}} N_{\alpha''}^0 \mathcal{X}'_{\alpha''\alpha\alpha'}], \quad (17)$$

$$E_{3x,\alpha\alpha'} = \sum_{\alpha''} [(1 + k_{\text{st}} N_{\alpha''}^0) e^{(\omega' + \omega - \omega'')/T} \mathcal{X}'_{\alpha'\alpha\alpha''} + k_{\text{st}} N_{\alpha''}^0 e^{(\omega' + \omega - \omega'')/T} \mathcal{X}'_{\alpha''\alpha\alpha'}] - k_{\text{st}} F_{3x,\alpha\alpha'}. \quad (18)$$

The linearization of the two-photon emission process scattering terms gives the following results: for the direct process 1y terms,

$$Q_{1y,\alpha}^0 = \sum_{\alpha'} N_{\alpha'}^0 \sum_{\alpha''} N_{\alpha''}^0 e^{(\omega' + \omega'' - \omega)/T} \mathcal{Y}_{\alpha\alpha'\alpha''}, \quad (19)$$

$$\kappa_{1y,\alpha}^0 = \sum_{\alpha'} (1 + k_{\text{st}} N_{\alpha'}^0) \sum_{\alpha''} (1 + k_{\text{st}} N_{\alpha''}^0) \mathcal{Y}_{\alpha\alpha'\alpha''} - k_{\text{st}} Q_{1y,\alpha}^0, \quad (20)$$

$$F_{1y,\alpha\alpha'} = \sum_{\alpha''} N_{\alpha''}^0 e^{(\omega' + \omega'' - \omega)/T} (\mathcal{Y}_{\alpha\alpha'\alpha''} + \mathcal{Y}_{\alpha\alpha''\alpha'}), \quad (21)$$

$$E_{1y,\alpha\alpha'} = k_{\text{st}} \sum_{\alpha''} (1 + N_{\alpha''}^0) (\mathcal{Y}_{\alpha\alpha'\alpha''} + \mathcal{Y}_{\alpha\alpha''\alpha'}) - k_{\text{st}} F_{1y,\alpha\alpha'}; \quad (22)$$

for the inverse 2y terms,

$$Q_{2y,\alpha}^0 = \sum_{\alpha'} (1 + k_{\text{st}} N_{\alpha'}^0) \sum_{\alpha''} N_{\alpha''}^0 \mathcal{Y}_{\alpha''\alpha'\alpha}, \quad (23)$$

$$\kappa_{2y,\alpha}^0 = \sum_{\alpha'} N_{\alpha'}^0 \sum_{\alpha''} (1 + k_{\text{st}} N_{\alpha''}^0) e^{(\omega + \omega' - \omega'')/T} \mathcal{Y}_{\alpha''\alpha'\alpha} - k_{\text{st}} Q_{2y,\alpha}^0, \quad (24)$$

$$F_{2y,\alpha\alpha'} = 12 \sum_{\alpha''} [(1 + k_{\text{st}} N_{\alpha''}^0) \mathcal{Y}_{\alpha''\alpha'\alpha} + k_{\text{st}} N_{\alpha''}^0 \mathcal{Y}_{\alpha''\alpha'\alpha}], \quad (25)$$

$$E_{2y,\alpha\alpha'} = \sum_{\alpha''} [(1 + k_{\text{st}} N_{\alpha''}^0) e^{(\omega + \omega' - \omega'')/T} \mathcal{Y}_{\alpha''\alpha'\alpha} + k_{\text{st}} N_{\alpha''}^0 e^{(\omega + \omega'' - \omega')/T} \mathcal{Y}_{\alpha''\alpha'\alpha}] - k_{\text{st}} F_{2y,\alpha\alpha'}; \quad (26)$$

and last, the linearized expressions for the 3y terms (i.e., photon exchange of the inverse),

$$Q_{3y,\alpha}^0 = \sum_{\alpha'} (1 + k_{\text{st}} N_{\alpha'}^0) \sum_{\alpha''} N_{\alpha''}^0 \mathcal{Y}_{\alpha''\alpha'\alpha}, \quad (27)$$

$$\kappa_{3y,\alpha}^0 = \sum_{\alpha'} N_{\alpha'}^0 \sum_{\alpha''} (1 + k_{\text{st}} N_{\alpha''}^0) e^{(\omega' + \omega - \omega'')/T} \mathcal{Y}_{\alpha''\alpha'\alpha} - k_{\text{st}} Q_{3y,\alpha}^0, \quad (28)$$

$$F_{3y,\alpha\alpha'} = \sum_{\alpha''} [(1 + k_{\text{st}} N_{\alpha''}^0) \mathcal{Y}_{\alpha''\alpha'\alpha} + k_{\text{st}} N_{\alpha''}^0 \mathcal{Y}_{\alpha''\alpha'\alpha}], \quad (29)$$

$$E_{3y,\alpha\alpha'} = \sum_{\alpha''} [(1 + k_{\text{st}} N_{\alpha''}^0) e^{(\omega' + \omega - \omega'')/T} \mathcal{Y}_{\alpha''\alpha'\alpha} + k_{\text{st}} N_{\alpha''}^0 e^{(\omega'' + \omega - \omega')/T} \mathcal{Y}_{\alpha''\alpha'\alpha}] - k_{\text{st}} F_{3y,\alpha\alpha'}. \quad (30)$$

### 3. RESULTS FOR ACCRETING X-RAY PULSARS

The earliest work that solved in some detail the radiative transport equation to simulate the emission from the accretion cap of an AXP binary is that of Nagel (1980, 1981a, b). He used nonrelativistic free-free and one-photon Compton scattering cross sections and a linear Feautrier scheme to calculate the emitted flux in the two-stream approximation. The polarizability of the plasma was included so that the transfer equation was solved for two normal modes for either slab or cylinder geometries with homogeneous temperature and density. These calculations were extended in Mészáros & Nagel (1985a, b) to include the effects of vacuum polarization and multiangle scattering. They solved the radiative transport equation for a discrete set of eight angles, 32 frequencies, and two polarization modes for slab and cylinder geometries and various external illumination scenarios. A representative set of conditions that give a good semblance of the Hercules X-1 spectrum consists of a self-radiating optically thick slab with homogeneous temperature  $T = 8$  keV, density  $\rho = 0.5$  g cm $^{-3}$ , cyclotron frequency  $\omega_c = 38$  keV, and slab thickness  $R = 10^5$  cm, which is essentially a semi-infinite atmosphere. These conditions correspond to a Thomson optical depth  $\tau_T = n_e \sigma_T R = \rho \sigma_T R / m_p = 2 \times 10^4$ , where  $m_p$  is the proton mass. The boundary conditions used were a free boundary at the top of the slab, reflection at the bottom, and no injected spectrum at either boundary.

The results of Mészáros & Nagel (1985a, b) give fair agreement with the time-averaged flux of Hercules X-1 (see Trümper et al. 1978 or White et al. 1983), but several problems still remain. The shape of the line is similar to an emission-line fit for the observed data with a cyclotron energy at  $\sim 55$  keV (see Voges et al. 1982); however, for the optical depth considered, the calculated line is in absorption, and with only one harmonic the blue shoulder of this comes out rather broad. In addition, for a high optical depth, stimulated effects will be important, so that the flux should saturate to the Planck instead of the Wien spectrum. Finally, their calculated flux can only be considered accurate for  $\omega \lesssim 1.5\omega_c$ , since the scattering cross sections that they used included only the effects of the first cyclotron harmonic. Above this frequency, the effects of the higher harmonics will determine the shape of the flux spectrum.

As was seen in Paper I, the opacity at the second and third harmonics is dominated by the two-photon scattering and emission processes. Since these are nonlinear, their inclusion in a Feautrier radiative transport calculation, which requires a linearization and iteration procedure, has not been solved previously. In this section the multiple photon scattering opacities and sources are included with the one-photon and free-free processes to study the characteristics of the higher cyclotron spectral features. All of the plasma parameters are the same as those used by Mészáros & Nagel (1985a, b) in their self-emitting slab model, and the opacities and sources are calculated up to the third harmonic (i.e., the same as the plots presented in Paper I). In addition, photons are created by free-free emission in an identical manner to that in the model of Mészáros & Nagel. In the present work, the inclusion of the multiple photon scattering processes puts severe limits on both computation time and memory, so that the calculations will be limited to the two-stream approximation for a grid of 32 frequencies.

As a first approximation, and as a starting solution for the nonlinear iterations, the case with linear one-photon Compton scattering including the second and third harmonics is calculated. The scattering opacity and source used in this model are identical

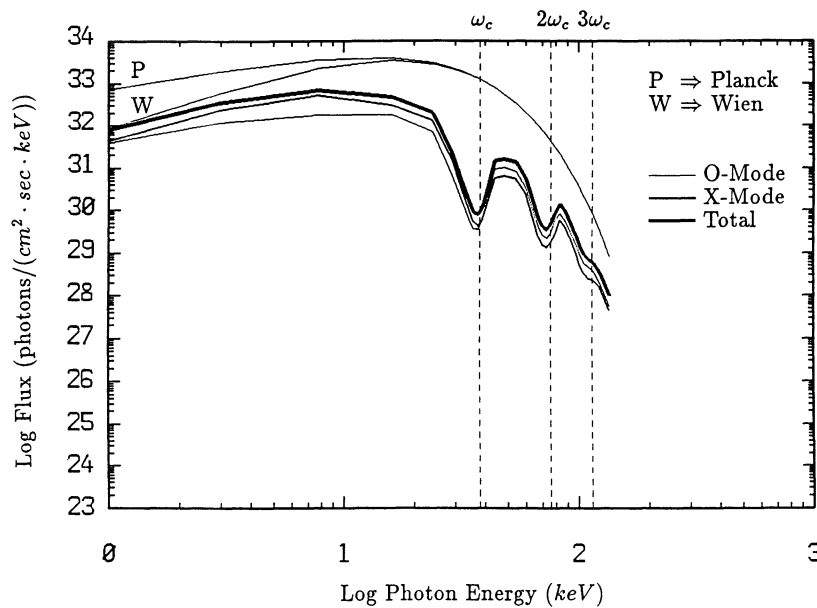


FIG. 1.—AXP flux spectrum using only one-photon scattering for the first three cyclotron harmonics. Stimulated effects are neglected.

to those in Figure 4 of Paper I and are given by equations (3)–(6). Of course, the source that is used during the calculations is determined by the actual radiation field. Figure 1 shows the emitted flux spectrum for such a calculation. The line at  $\omega_c$  is similar to that in Mészáros & Nagel (1985a, b), while here a line appears at  $2\omega_c$  and no line at  $3\omega_c$ . The observed spectrum of Hercules X-1 of Trümper et al. (1978) spans several orders of magnitude in flux, and photons are recorded in the energy range  $10 \text{ keV} \lesssim \omega \lesssim 150 \text{ keV}$ . The flux sensitivity of the instrument can be estimated to be  $\sim 3.5$  orders of magnitude below the flux level of the shoulder at an energy  $\omega \sim 20 \text{ keV}$ , which corresponds to a flux of  $\sim 10^{29} \text{ photons cm}^{-2} \text{ keV}^{-1} \text{ s}^{-1}$  in Figure 1 (at the source). The calculated one-photon line at  $2\omega_c$  is completely above this flux limit; and thus one would expect that the second harmonic line should have been completely resolved. The more recent observations of Hercules X-1 in Mihara et al. (1990) extend only to photon energies  $\omega \sim 60 \text{ keV}$ , but they do show a sharp decrease in flux for  $\omega > 50 \text{ keV}$  which is not evident in Figure 1. This implies that the calculated flux in Figure 1 is not correct and that there must be other processes, besides one-photon scattering, that determine the structure of the higher cyclotron lines.

The radiation field of Figure 1 can be used as a starting solution for a nonlinear calculation including the multiple photon processes. Equations (7)–(18) contain the linearized discrete ordinate forms of the sources and opacities for the two-photon scattering, while those for the two-photon emission are in equations (19)–(30). As a first example, the two-photon processes are included without stimulated factors (i.e.,  $k_{st} = 0$ ). Figure 2 shows the total flux emitted from the top of the slab for the starting

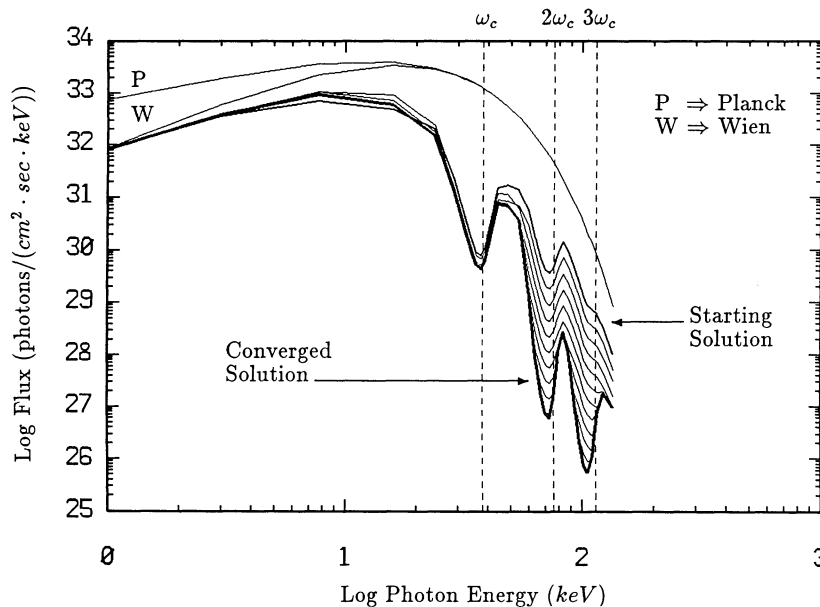


FIG. 2.—AXP total flux spectra for each iteration of the nonlinear calculation that includes one-photon and two-photon processes for the first three cyclotron harmonics. The starting solution is the radiation field of Fig. 1, and stimulated effects are neglected.

conditions, the converged solution, and each iteration in between. The starting solution is the linear calculation of Figure 1, and one sees that with successive iterations the lines are formed at  $2\omega_c$  and  $3\omega_c$ , and the flux converges in 18 iterations, where the criterion for convergence is  $\delta N_\alpha/N_\alpha^0 < 10^{-6}$  for all  $\alpha$ . As the iterations proceed, the second and third harmonics get stronger, and the photons spawned there reappear in the neighborhood of the first harmonic. For this very high optical depth, however, the one-photon Compton process at the first harmonic is very efficient in scattering these photons out into the low-energy wing, where one sees a gradual buildup of the continuum.

Figure 3 shows the converged calculated flux spectrum for each polarization mode and the total. Including the multiple photon scattering does not affect the line at  $\omega_c$  significantly; however, the flux at  $2\omega_c$  and  $3\omega_c$  is completely dominated by these processes. The reason for the drastic increase in line depth is found in the different behavior between one-photon scattering and two-photon scattering and emission. In the one-photon case, even for several scatterings, photons are not redistributed very far from the line core. On the other hand, both the two-photon scattering and emission processes redistribute photons directly from the higher harmonics to the lower. For example, in the one-photon case, an incident photon with  $\omega \sim 2\omega_c$  will scatter to a final photon of approximately the same energy; but in the case of two-photon scattering or emission, the same incident photon will scatter into two photons with  $\omega \sim \omega_c$ , which will then scatter into the line wings. Thus, since the cross sections for the two-photon processes exceed that for the one-photon near the second harmonic, photons at  $\omega \sim 2\omega_c$  are depleted, while those at  $\omega \sim \omega_c$  are replenished. The net result is that the spectral line at the higher harmonics will become significantly deeper than with just one-photon scattering.

How does the calculated flux of Figure 3 compare with the observations of Hercules X-1? The line at  $\omega_c$  is essentially unchanged from previous calculations and shows good agreement. The rapid decrease in flux for  $\omega \gtrsim 50$  keV that is evident in Figure 3 is consistent with similar decreases reported in Trümper et al. (1978) and Mihara et al. (1990). The flux sensitivities for these two observations are estimated to be  $\sim 10^{29}$  photons  $\text{cm}^{-2}$   $\text{keV}^{-1}$   $\text{s}^{-1}$  and  $\sim 10^{28}$  photons  $\text{cm}^{-2}$   $\text{keV}^{-1}$   $\text{s}^{-1}$  (at the radiating site), respectively; so according to Figure 3, neither observation could have resolved the line at  $2\omega_c$ .

For high optical depths, stimulated effects can increase the flux near the cyclotron lines. If the calculations for Figure 3 are repeated with  $k_{\text{st}} = 1$  in all of the opacities and sources, the emitted flux is calculated as shown in Figure 4. Comparing this plot with Figure 3, the relative shapes and locations of the cyclotron lines are unchanged; however, including stimulated factors causes a factor of 2 increase in the flux in the region of the cyclotron harmonics. This flux is still consistent with the observations of Hercules X-1 and shows the rapid flux decrease for  $1.5\omega_c < \omega < 2\omega_c$ . Since this calculation includes all of the relevant physics considered in this work, it probably represents a fairly accurate representation of the cyclotron line formation process within this model. Note that the degree of polarization of the continuum and the harmonics is very significant, depending sensitively on the total optical depth. The line flux at the first harmonic is a factor  $\sim 10^{2.5}$  below the flux at the shoulder at  $\omega \sim 20$  keV where the power-law slope changes. The width of the line is estimated to be  $W \sim 11$  keV. The flux for the  $2\omega_c$  line is  $\sim 10^{2.8}$  less than that at  $\omega_c$ , and it has a width  $W \sim 18$  keV. The third harmonic line has a flux depth  $\sim 10^1$  less than the second, or  $\sim 10^{3.8}$  below the first, and a width  $W \sim 24$  keV. Mihara et al. (1990) fit their data to an absorption model and obtain a width of  $W \sim 12 \pm 2$  keV for the first harmonic line. Since the other lines have never been resolved, the characteristics calculated here remain a prediction.

#### 4. RESULTS FOR GAMMA-RAY BURSTERS

In this section we expand on the results for GRBs reported in Alexander & Mészáros (1989). In that letter, we presented calculations for a model that demonstrated how the quantum electrodynamics (QED) opacities determine the shape of the cyclotron lines in the X-ray portion of the spectrum of a GRB, as seen in the *Ginga* observations and reported in Murakami et al. (1988). The

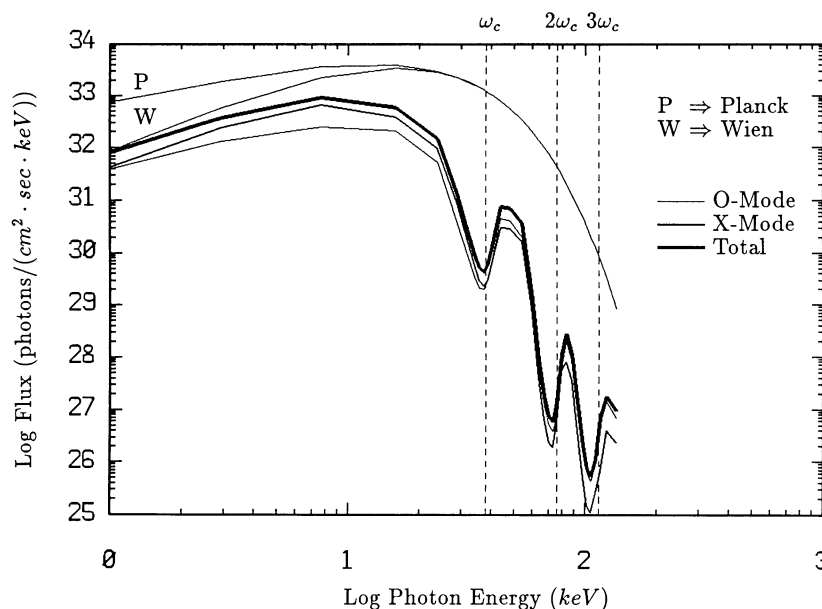


Fig. 3.—AXP flux spectrum using one-photon and two-photon processes for the first three cyclotron harmonics. Stimulated effects are neglected.

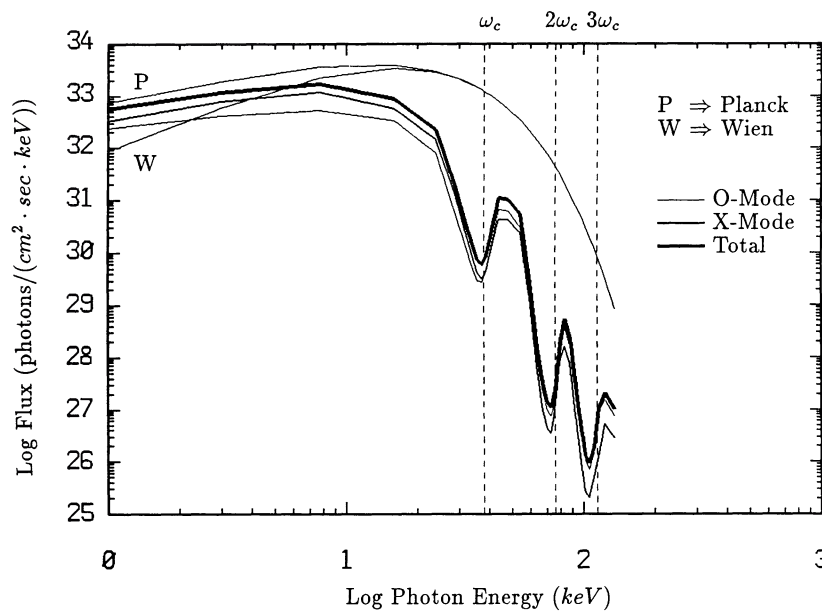


FIG. 4.—AXP flux spectrum using one-photon and two-photon processes for the first three cyclotron harmonics. Stimulated effects are included.

model consists of an optically thin sheet of plasma distinct from the gamma-ray-emitting region that is threaded by a strong magnetic field, as in Fenimore et al. (1988) and Wang et al. (1989b). Photons from the burst event pass through the sheet, and scattering from the electrons creates the cyclotron lines. Computationally, this can be modeled as a uniform slab with a patched power-law spectrum of incident unpolarized radiation on the lower boundary. For a more complete background and discussion of this calculation, see Alexander & Mészáros (1989) and references therein.

In our previous work, we included only one-photon and two-photon scattering, and by varying the optical thickness of the slab we found that cyclotron lines comparable to those observed could be calculated. Here we wish to extend this treatment to include also the effects of the two-photon emission process. These updated results, presented below, do not differ qualitatively from our previous ones in the structure of the cyclotron lines; however, the required optical depth to obtain agreement with observations is different.

Based on the observations of GB 880205, Fenimore et al. (1988) suggest the plasma parameters for the sheet: temperature  $T = 5.2$  keV, density  $\rho = 6 \times 10^{-4}$  g cm<sup>-3</sup>, in a magnetic field normal to the slab with cyclotron frequency  $\omega_c = 20$  keV. Figure 5 shows our calculated total flux spectra for these conditions and three slab thicknesses for an angle relative to the field of  $60^\circ$  (previously we found that  $60^\circ$  gives us the best agreement with the observed flux). These plots are similar to Figure 2 in Alexander & Mészáros

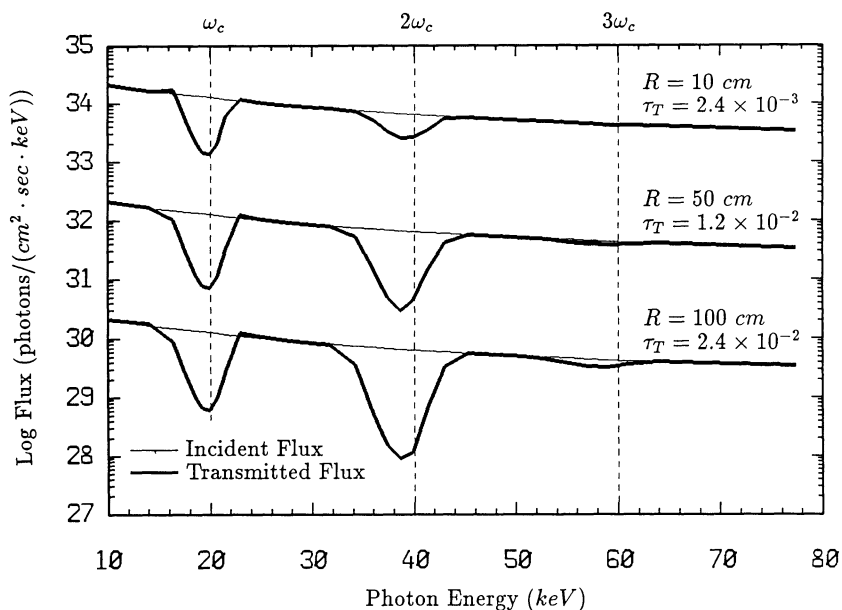


FIG. 5.—GRB total flux spectra for three values of the sheet thickness. The light line is the input spectrum. For clarity, the uppermost and lowest curves are offset by a factor of 100 up and down with respect to the middle one.

(1989). The frequency grid consists of 32 frequencies, as in § 3; the depth and shape of the lines do not change significantly with an increase in the number of grid points. In the present Figure 5, however, the additional process of two-photon emission is included in the calculations. We see that this additional scattering causes the cyclotron lines to form at lower optical depths than our previous calculations that included only one- and two-photon scattering. The observed spectrum exhibits roughly equal depth lines from the continuum at the first and second harmonics and possibly a very shallow line at the third harmonic. Figure 5 suggests that lines of this nature could be achieved for an optical depth between the upper two plots. Figure 6 shows the calculated flux spectrum for a slab thickness of 45 cm which corresponds to a Thomson optical depth of  $\tau_T \sim 1.1 \times 10^{-2}$ . Note that this best-fit optical depth is a factor of 2 less than our previous result in Alexander & Mészáros (1989), where two-photon emission was not included. Notice that the addition of two photon emission changes the line flux and the required optical depth by a factor which is not directly proportional to the change in the opacity. This is because the two-photon emission (like the two-photon scattering) is nonlinear, with an optical depth larger than unity in the lines, and thus a detailed radiative transfer calculation leads to a nonlinear change in the optical depth. In addition, since the optical depth of the slab is lower than for our previous result, the degree of linear polarization of the radiation at the lines is different. Now we have  $\sim 30\%$ ,  $\sim 80\%$ , and  $\sim 10\%$  linear polarization for the lines at  $\omega_c$ ,  $2\omega_c$ , and  $3\omega_c$ , respectively.

### 5. DISCUSSION

The results presented in the previous sections indicate the need for the inclusion of the various nonlinear effects in a radiative transfer calculation, in particular the two-photon processes. This is especially important for the treatment of those spectral regions where the optical depth is higher, e.g., at the cyclotron resonances, where the photon occupation number is high. Comparing the AXP results of Figure 1 (without two-photon processes) and Figure 3 (which includes two-photon scattering, two-photon emission, and their inverses), one sees that the latter processes introduce a major change in the line fluxes, even at the first harmonic. This amounts in this example to about half an order of magnitude at the first harmonic dip, and one order of magnitude in the first harmonic blue shoulder. It is more than two orders of magnitude at the higher harmonics. The GRB results of Figures 5 and 6 also show that the inclusion of these nonlinear, two-photon effects changes the required optical depth significantly.

We have also performed calculations where we included two-photon scattering but not two-photon emission. In these, significant flux differences compared with the case of one-photon scattering were also present, as expected from the fact that these two processes have somewhat similar cross sections (Paper I). The flux differences in this case are less extreme than those shown here between Figure 1 and Figure 3, which contains both two-photon processes. Because of the nonlinearity of the transfer equations in the presence of a multiple-photon process, and the different frequency behavior, adding the two-photon emission to the two-photon scattering translates into a flux which is different by a larger factor. This is evident also in the GRB results of Figures 5 and 6, where the inclusion of two-photon emission in addition to two-photon scattering decreased by a factor of 2.2 the slab depth required to explain the line ratios, compared with Alexander & Mészáros (1989). Because the detailed frequency dependence of the two-photon emission is different (e.g., no continuum contribution), and the increased nonlinear behavior leads to a larger flux change, both of these two-photon processes must be used simultaneously in the radiative transfer code to obtain the self-consistent line strengths and ratios.

The effect of including stimulated processes, another nonlinear effect, is to increase somewhat the flux at the cyclotron harmonics, as shown in Figure 4. This is the opposite of the tendency noted by Alexander et al. (1989) for the case of stimulated effects in the

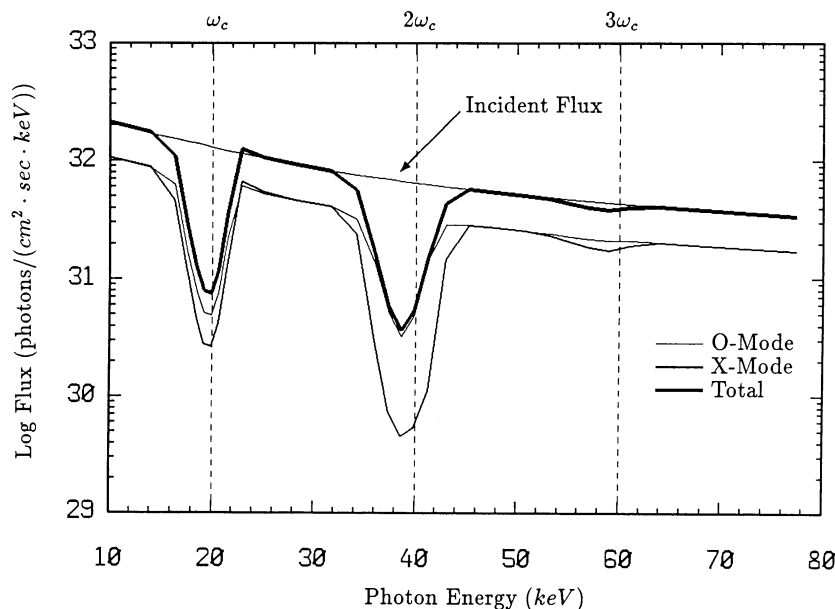


FIG. 6.—GRB flux spectra for a sheet of thickness 45 cm or  $\tau_T \simeq 1.1 \times 10^{-2}$ , showing the input spectrum, the total spectrum, and separately also the polarization 1 (X) and polarization 2 (O) components.

one-photon scattering at the first harmonic. However, in that work, the effect of stimulated scattering was compared with calculations that included stimulated factors in the free-free processes but not in the scattering. Here we compare the calculation with all stimulated factors with the case where none are present. The effect of the stimulated processes is not as pronounced as that of including the two-photon scattering and emission, because the latter redistribute photons from the higher harmonics to the ground. However, stimulated scattering is nonetheless important for obtaining the correct order of magnitude of the fluxes at the higher harmonics, and is responsible for corrections by factors of a few near the first harmonic, in a high optical depth case. In the low optical depth GRB case, however, the stimulated effects are very small.

The calculations described here use the two-stream approximation, and the angle was chosen in the GRB example to give a line width comparable to the GB 880205 observations. The two-stream approximation corresponds to an angle-averaged spectrum, and should be fairly accurate when the optical thickness is large. This is the case for the AXP model discussed here; in the GRB model, however, this is true only in the first and second harmonic line cores but not in the wings. Our GRB third harmonic line depths are therefore only approximate. Also, within a two-stream calculation, a numerical fit to the actual observed data would involve varying  $T_e$  and  $\theta$  as well as the slab depth  $\tau_T$ . However, our purpose here has been to investigate the dependence on the physical effects, rather than to perform such a detailed fit. Because of this, derived parameters such as the optical depths discussed here are not absolute values but serve to illustrate the sensitivity of the results to the inclusion of the various processes.

The AXP results of Figure 4 are accurate from a physical point of view, although they are obtained for a very simplified atmosphere, which ignores questions of energetics and dynamics as well as general relativistic complications. Nonetheless, the parameters used are close to what one may expect on average for a source like Hercules X-1. The calculations show that one does not expect the observations of Trümper et al. (1978) and Voges et al. (1982) to have detected a second harmonic, as indeed they did not. A first harmonic was tentatively identified in the first flight of these observations, but was not seen in the later flights with higher sensitivity by the same group. On the other hand, it is important to note that the second harmonic does have an important role in lowering and steepening the blue shoulder of the first harmonic. For instance, if one does not include a second harmonic, as in the nonrelativistic calculations of Mészáros & Nagel (1985a), the blue shoulder of the first harmonic "absorption" (i.e., outscattering) feature is higher than the observations warrant. This is also confirmed by the results of Mihara et al. (1990), who obtain a good fit to their *Ginga* observations of Hercules X-1 by using two harmonics, even though the second is just outside the instrument sensitivity range, which provides the appropriate steep falloff above the blue shoulder.

A prediction of these radiative transfer calculations is that the flux at the cyclotron harmonics should be highly polarized. For accreting X-ray pulsars, as seen in Figure 4, which shows the ordinary and extraordinary polarization modes separately, one expects the ordinary mode to dominate in general. The ordinary mode is the one that has the electric vector in the plane of the magnetic axis and observer direction, or rotation sense contrary to that of the electron. One can estimate the polarization degree at the second harmonic to be upward of 30%–40%, and at the third upward of 80%. These values depend sensitively on the optical depth, and as such will depend on the details of the fit to the data. An inhomogeneous atmosphere may cause these estimates to be lowered, but the degree of polarization is still expected to remain very substantial. Such predictions for accreting pulsars of moderate magnetic field strength should be testable by the soft X-ray polarimeter (SXP) to be flown on the *Spectrum X-Gamma* mission (e.g., Kaaret et al. 1990). For gamma-ray bursters, as shown in Figure 6, it is similarly the ordinary mode that dominates the lines, at least if the incident continuum is unpolarized, as assumed here. The degree of polarization caused by the two-photon scattering and emission processes on this continuum at the lines is  $\sim 30\%$ ,  $\sim 80\%$ , and  $\sim 10\%$  in the first, second, and third harmonics, respectively, for an object like GB 880205.

This research has been supported in part through grants NASA NAGW-1522 and NSF AST 8815266.

#### REFERENCES

- Alexander, S. G., & Mészáros, P. 1989, *ApJ*, 344, L1  
 ———. 1990a, *BAAS*, 21 (No. 4), 1175  
 ———. 1990b, *ApJ*, 372, 554 (Paper I)  
 Alexander, S. G., Mészáros, P., & Bussard, R. W. 1989, *ApJ*, 342, 928  
 Bussard, R. W., Alexander, S. G., & Mészáros, P. 1986, *Phys. Rev. D*, 34, 440  
 Bussard, R. W., Mészáros, P., & Alexander, S. G. 1985, *ApJ*, 297, L21  
 Chandrasekhar, S. 1960, *Radiative Transfer* (New York: Dover)  
 Clark, G. W., Woo, J. W., Nagase, F., Makishima, K., & Sakao, T. 1990, *ApJ*, 353, 274  
 Daugherty, J., & Harding, A. K. 1986, *ApJ*, 309, 362  
 Fenimore, E. E., et al. 1988, *ApJ*, 335, L71  
 Harding, A. K., & Preece, R. 1989, *ApJ*, 338, L21  
 Kaaret, P., et al. 1990, in *IAU Colloquium 123, Observatories in Earth Orbit and Beyond*, in press  
 Makishima, K., et al. 1991, *ApJ*, 365, L59  
 Mazets, E. P., et al. 1982, *Nature*, 290, 378  
 Mészáros, P., & Nagel, W. 1985a, *ApJ*, 298, 147  
 ———. 1985b, *ApJ*, 299, 138  
 Mihara, T. et al. 1990, *Nature*, 346, 250  
 Murakami, T., et al. 1988, *Nature*, 335, 234  
 Nagase, F., et al. 1991, *ApJ*, submitted  
 Nagel, W. 1980, *ApJ*, 236, 904  
 ———. 1981a, *ApJ*, 251, 278  
 ———. 1981b, *ApJ*, 251, 288  
 Roussel-Dupré, D., et al. 1990, *BAAS*, 21 (No. 4), 1204  
 Trümper, J., Pietsch, W., Reppin, C., Voges, W., Staubert, R., & Kendziorra, E. 1978, *ApJ*, 219, L105  
 Voges, W., Pietsch, W., Reppin, C., Trümper, J., Kendziorra, E., & Staubert, R. 1982, *ApJ*, 263, 803  
 Wang, J. C., Wasserman, I., & Salpeter, E. E. 1988, *ApJS*, 68, 735  
 ———. 1989a, *ApJ*, 338, 343  
 Wang, J. C., et al. 1989b, *Phys. Rev. Letters*, 63, 1550  
 Wheaton, W., et al. 1979, *Nature*, 282, 240  
 White, N. E., Swank, J. H., & Holt, S. S. 1983, *ApJ*, 270, 711  
 Yoshida, A., et al. 1990, in *Los Alamos Workshop on Gamma-Ray Bursts*, ed. R. Epstein, E. Fenimore, & C. Ho (Cambridge: Cambridge Univ. Press), in press